Tailored B_1 Mapping for Multi-Element Transmit Applications

K. Nehrke[1], and P. Börnert[1]

[1]Philips Research Europe, Hamburg, Germany

Introduction

Accurate B_1-mapping is an essential prerequisite for multi-element transmit applications [1,2] like e.g. RF-shimming or multi-dimensional RF pulse design. However, in vivo B_1-mapping is still challenging with respect to scan time and mapping accuracy. Recently, a matrix approach for B_1-mapping has been proposed [3,4] to avoid adverse error propagation in the limit of low flip-angles. In the present work, this concept is extended to tailor the transmit channel encoding matrix used for the mapping scan with respect to the chosen application. This approach is essentially equivalent to the transformation of the problem to an appropriate virtual coil array. The underlying theory will be briefly outlined, and basic feasibility will be evaluated on phantoms and in-vivo.

Theory

The coil sensitivities **S** of a transmit array can be given by its singular value decomposition (SVD) $\mathbf{S}=\mathbf{U\Sigma V}^H$. The columns of **S** form vectors that contain the spatial sensitivities of the *N* individual Tx coils. The orthogonal matrix **V** represents a transformation from the *N* physical coil elements to the *N* normal (eigen) modes of the coil arrays, represented by their orthonormal transmit sensitivities stored in the columns of the matrix **U**. The *N* singular values σ_i, held by the diagonal matrix $\mathbf{\Sigma}$, describe the conditioning of the coil array with respect to its normal modes. Hence, eigen-modes with small singular values will be determined less precisely by the mapping scan. Since the SVD is a unique transformation, the singular values are fixed hardware parameters of the given coil array. However, this limitation can be overcome for the B_1 mapping scan by measuring the maps with respect to a virtual coil system $\mathbf{S}'$ described by the transformation $\mathbf{S}'=\mathbf{SE}$. Here, **E** denotes the encoding matrix, which is now chosen as $\mathbf{E}=\mathbf{V\Gamma V}^H$, where $\mathbf{\Gamma}$ is a diagonal matrix with the entries γ_i. The SVD of $\mathbf{S}'$ is then given by $\mathbf{S}'=\mathbf{U\Sigma\Gamma V}^H$, and the singular values of the virtual coil system are $\sigma'_i=\gamma_i\,\sigma_i$. Hence, the eigenvalues γ_i of the encoding matrix can be chosen to tailor σ'_i according to the desired application. For example, γ_1 could be increased to further emphasize the primary coil mode (uniform mode) for noise suppression in the maps [3,4]. Moreover, the conditioning of the coil array could be improved by balancing the higher modes. For a cylindrical coil array, the circular symmetry results in particularly simple properties. The orthogonal matrix **V** is then given by the discrete Fourier transform [5], which, in turn, leads to a circulant encoding matrix **E** (i.e. cyclically shifted row vectors) with only *N* independent weights.

Methods

Phantom and in vivo experiments (five healthy volunteers) were performed on a 3T MRI system (Philips Medical Systems, Best, The Netherlands) equipped with eight transmit channels [6] and an 8-element TX/RX body coil [7]. The AFI (Actual Flip Angle Imaging) technique [8] was used for B_1 mapping (450 mm FOV, 128 scan matrix, flip-angle = 60°, TR_1 = 20 ms, TR_2 = 100 ms). Three different encoding schemes were investigated for a cylindrical oil phantom (∅= 400 mm): A) conventional ($\gamma_{1\ldots8}=1$), B) all-but-one [3] ($\gamma_1=-\sqrt{7}$, $\gamma_{2\ldots8}=1/\sqrt{7}$), C) balanced scheme with emphasized higher modes ($\gamma_{1\ldots8}$= -2.3, 0.14, 0.19, 0.26, 0.38, 0.55, 0.8, 1.2). The maximum power per coil element was kept constant to facilitate comparison. In vivo B_1 maps of the pelvis were acquired and used for RF shimming. Two different encoding schemes (conventional and all-but-one) were compared.

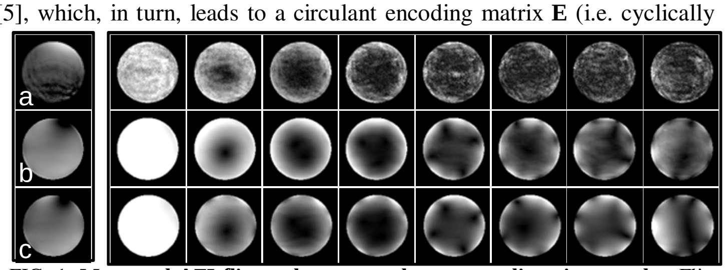

FIG. 1. **Measured AFI flip-angle maps and corresponding eigen-modes.** Flip-angle maps of one virtual coil element are shown for three different encoding schemes (left frame, a: conventional, b: all-but-one, c: balanced). The remaining elements have been omitted because of the circular symmetry. The right frame shows the corresponding orthonormal modes (1-8 from left to right) obtained by singular value decomposition (SVD). Note the different noise characteristics for the different encoding schemes.

Results

The conventional encoding (A) resulted in significant noise in the maps, spoiling especially the contributions from the higher coil eigen-modes almost completely (Fig.1). In contrast, the all-but-one encoding (B) yielded only moderate noise due to the increased weight of the uniform mode. The balanced scheme (C) further improved the quality of the higher modes (5-8) on cost of the lower modes (2-4) as a result of the balanced weights. Similarly, in the in vivo experiments, the all-but-one scheme yielded a better quality than the conventional one (Fig.2). Accordingly, the all-but-one scheme resulted in more reliable shimming results.

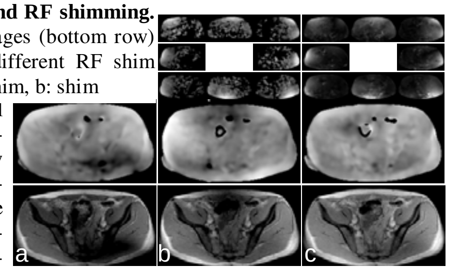

FIG. 2. **In vivo B_1 mapping and RF shimming.** B_1 maps (middle row) and images (bottom row) of the pelvis obtained with different RF shim settings are shown (a: default shim, b: shim derived from conventional maps, c: shim derived from all-but-one maps). The top row shows the corresponding multi-channel maps. The all-but-one maps were transformed to single coil maps to facilitate comparison.

Discussion

The presented approach allows the conditioning of a transmit coil array in a B_1 mapping scan to be tailored with respect to the chosen application. Emphasizing the uniform mode helps to eliminate regions with low B_1, and hence, to suppress noise in the maps. This potentially improves the performance of multi-element transmit applications. Additional balancing of the remaining modes could be important for demanding applications such as e.g. design of accelerated multi-dimensional RF pulses [1,2], posing higher requirements on the mapping accuracy of all coil modes.

References

1. Katscher U et al. Magn Reson Med. 2003;49(1):144-50.
2. Zhu Y. Magn Reson Med. 2004;51(4):775-84.
3. Nehrke K and Börnert P. ISMRM 2008, p.353.
4. D. O. Brunner and K. P. Pruessmann. ISMRM 2008, p.354.
5. Mispelter J. et al. NMR probeheads. Imperial College Press, 2006
6. Grässlin I et al., ISMRM 2006, p.129.
7. Vernickel P et al. Magn Reson Med. 2007;58:381-9.
8. Yarnykh VL. Magn Reson Med. 2007;57(1):192-200.